

Synthesis and Characterization of the Cerium(III) UV-Emitting 2D-Coordination Polymer $\frac{2}{\infty}[\text{Ce}_2\text{Cl}_6(4,4'\text{-bipyridine})_4]\cdot\text{py}$

Philipp R. Matthes^[a] and Klaus Müller-Buschbaum^{*[a]}

Dedicated to Professor Martin Jansen on the Occasion of His 70th Birthday

Keywords: Coordination polymers; Cerium; MOFs; Luminescence; 4,4'-Bipyridine

Abstract. The 2D-coordination polymer $\frac{2}{\infty}[\text{Ce}_2\text{Cl}_6(\text{bipy})_4]\cdot\text{py}$ (bipy = 4,4'-bipyridine) shows a 5d-4f centered emission in the soft UV-B region. It was synthesized via the reaction of anhydrous CeCl_3 and 4,4'-bipyridine in pyridine under solvothermal conditions. The two-dimensional sheet structure consisting of 4,4'-bipyridine coordinated Ce_2Cl_6 dimers closes the gap between the known lanthanum $\frac{3}{\infty}[\text{La}_2\text{Cl}_6(\text{bipy})_5]\cdot 4\text{bipy}$ framework and the 2D networks of the formula $\frac{2}{\infty}[\text{Ln}_2\text{Cl}_6(\text{bipy})_3]\cdot 2\text{bipy}$ from praseodymium on. They differ in

the number of coordinating bipy linkers, which decreases along $\text{La} > \text{Ce} > \text{Pr}$, with the remarkable observation that lanthanum, cerium, and praseodymium exhibit different network constitutions. The structure of $\frac{2}{\infty}[\text{Ce}_2\text{Cl}_6(\text{bipy})_4]\cdot\text{py}$ exhibits a *cem* topology constituted of double strands, which are diagonally linked by 4,4'-bipyridine forming trapezoid cavities in-between the strands. The cavities contain intercalated pyridine molecules.

Introduction

Metal-organic frameworks and coordination polymers^[1] show a wide diversity of physical properties like porosity,^[2] magnetism,^[3] and luminescence,^[4] which can be used for a variety of potential applications like gas-storage,^[5] sensor-development,^[6] and as light-converter^[7] materials. In recent years, the investigation and determination of the luminescent properties of these materials progressively moves into the focus of scientific interest. Ce^{III} -centred luminescence can be observed in purely lanthanide containing coordination polymers and MOFs^[8] as well as doped into lanthanide free host lattices.^[9] Cerium containing frameworks are still rare and are commonly accessed via solvothermal reactions of hydrated cerium salts with carboxylic acids. We were able to utilize a solvent free melt synthesis strategy to obtain coordination polymers and networks based on anhydrous lanthanide chlorides and dinitriles^[10] or 4,4'-bipyridine (bipy),^[11] bypassing quenching effects caused by coordinated ligands containing –OH or –NH functional groups.^[12] However, the solvent free approach is accompanied by a complex crystallization process, so that not all products obtained can be identified and characterized. The lanthanum containing 3D framework $\frac{3}{\infty}[\text{La}_2\text{Cl}_6(\text{bipy})_5]\cdot 4\text{bipy}$ ^[11a] and the 2D network $\frac{2}{\infty}[\text{Ln}_2\text{Cl}_6(\text{bipy})_3]\cdot 2\text{bipy}$,^[11b,11c] ($\text{Ln} = \text{Pr}, \text{Nd}, \text{Sm}, \text{Eu}, \text{Gd}, \text{Tb}$), mark examples with a significant structural difference and con-

stitution, whilst the intermediate with cerium was missing prior to this work.

Results and Discussion

In order to close this gap, the solvent free approach was modified by assisting solvents. Hereby, pyridine can be beneficial for crystallization due to the partial dissolution of LnCl_3 forming a small amount of reactive LnCl_3 -pyridine complexes, initially.^[13] Under solvothermal reaction conditions the coordinated pyridine can be replaced by bridging bipyridine molecules leading to an exclusively bipy-connected network based on CeCl_3 -SBUs (secondary building units). Accordingly, the reaction product marks the missing link between lanthanum and praseodymium, which can be achieved by the formation of the 2D coordination polymer $\frac{2}{\infty}[\text{Ce}_2\text{Cl}_6(4,4'\text{-bipy})_4]\cdot\text{py}$, presented herein.

Crystal Structure

The crystal structure of $\frac{2}{\infty}[\text{Ce}_2\text{Cl}_6(4,4'\text{-bipy})_4]\cdot\text{py}$ was determined on single crystals. It crystallizes in the monoclinic space group *C*/2m. Crystallographic data is presented in Table 1, selected interatomic distances can be found in Table 2. Trivalent cerium is found on one crystallographic site and exhibits a coordination number of eight, which is in-between lanthanum in $\frac{3}{\infty}[\text{La}_2\text{Cl}_6(\text{bipy})_5]\cdot 4\text{bipy}$ ^[11a] with five bipy per dimeric unit (C.N. = 8) and praseodymium in $\frac{2}{\infty}[\text{Ln}_2\text{Cl}_6(\text{bipy})_3]\cdot 2\text{bipy}$ ^[11b,11c] with three bipy per dimeric unit (C.N. = 7). Cerium is coordinated by four nitrogen atoms of four 4,4'-bipyridine molecules and four chloride ions, generating a dodecahe-

* Prof. Dr. K. Müller-Buschbaum
Fax: +49-931-3184785
E-Mail: k.mueller-buschbaum@uni-wuerzburg.de

[a] Universität Würzburg
Institut für Anorganische Chemie
Am Hubland
97074 Würzburg, Germany

dron as coordination sphere. Two cerium coordination spheres form a Ce_2Cl_6 dimer, which is edge connected by a bridge consisting of two μ_2 -chloride ions [$\text{Ce1}-\text{Cl3}$: 286.64(11) pm, $\text{Ce1}-\text{Cl3}^{\text{I}}$: 295.25(10) pm]. The other chloride ions are terminally bound to cerium [$\text{Ce1}-\text{Cl1}$: 278.27(12) pm, $\text{Ce1}-\text{Cl2}$: (274.16(13) pm)].

Table 1. Crystallographic data for $\frac{2}{3}[\text{Ce}_2\text{Cl}_6(4,4'\text{-bipy})_4]\cdot\text{py}$.

	$\frac{2}{3}[\text{Ce}_2\text{Cl}_6(4,4'\text{-bipyridine})_4]\cdot\text{py}$
Formula weight /g·mol ⁻¹	1196.91
Crystal system	monoclinic
Space group	<i>C2/m</i>
<i>a</i> /pm	1404.0(3)
<i>b</i> /pm	1225.3(3)
<i>c</i> /pm	1405.4(3)
β /°	92.27(3)
Volume /pm ³ × 10 ⁶	2415.8(8)
<i>Z</i>	2
d_c /g·cm ⁻³	1.6355
Diffractometer	Bruker SMART Apex I
X-ray radiation	Mo- <i>K</i> α (graphite monochromator)
Temperature /K	168(3)
2θ max /°	60.3
μ /mm ⁻¹	2.233
<i>F</i> (000)	1164
All reflections collected	18425
Independent reflections	3713
Data / restraints / parameters	3713/0/221
<i>S</i>	1.121
R_1 for <i>n</i> reflections [$I > 2\sigma(I)$] ^{a)}	0.0288
R_1 [all data] ^{a)}	0.0310
wR_2 [all data] ^{b)}	0.0700
Largest diff. peak/hole /(e pm ⁻³)·10 ⁻⁶	1.30/−0.78

a) $R_1 = \sum(|F_o| - |F_c|) / \sum|F_o|$. b) $wR_2 = \sum w(|F_o|^2 - |F_c|^2) / \sum w|F_o|^2$ ^{1/2}.

Table 2. Selected interatomic distances /pm for $\frac{2}{3}[\text{Ce}_2\text{Cl}_6(4,4'\text{-bipy})_4]\cdot\text{py}$.

Ce1	C11	278.27(12)	N2	C10A	138.1(6)
Ce1	C12	274.16(13)	N2	C6B	146.1(17)
Ce1	Cl3 ^I	295.25(10)	N2	C10B	112.0(15)
Ce1	Cl3	286.64(11)	C8	C8 ^{III}	148.6(6)
Ce1	N1 ^{II}	262.8(2)	C3	C3 ^{II}	149.2(6)
Ce1	N1	262.8(2)	range (C–N, C–C)		110(7)–145.1(19)
Ce1	N2 ^{II}	283.7(2)			
Ce1	N2	283.7(2)			

Symmetry operations: ^I1−*x*, *y*, 1−*z*; ^{II}*x*, −*y*, *z*; ^{III}3/2 −*x*, 1/2 −*y*, −*z*.

The dimeric unit is depicted in Figure 1. The Ce–Cl distances are in good agreement with the dimeric complex $[\text{CeCl}_2(\mu\text{-Cl})(\text{py}-(R,R)\text{-chxn})_2]$ ¹⁴ (terminal Ce–Cl 274.3–278.3 pm, bridging Ce–Cl 284.0–290.8 pm). All six chloride ions and both cerium atoms of the dimer are positioned on the *bc* plane. This structural motif has not yet been reported for other compounds based on lanthanide halides coordinated by pyridyl ligands.

Dinuclear species with double halide bridged lanthanides and a coordination number of eight can show out-of-plane coordination of the chloride anions, as found for $\text{Nd}_2\text{Cl}_6(1,10\text{-phenanthroline})_4$,¹⁵ $\text{La}_2\text{Cl}_6(\text{pyridine})_8$,^{13b)} and $\frac{3}{2}[\text{La}_2\text{Cl}_6(4,4'\text{-bipy})_5]\cdot 4(4,4'\text{-bipy})$ ^{11a)}. In $\frac{2}{3}[\text{Ce}_2\text{Cl}_6(4,4'\text{-bipy})_4]\cdot\text{py}$, the four

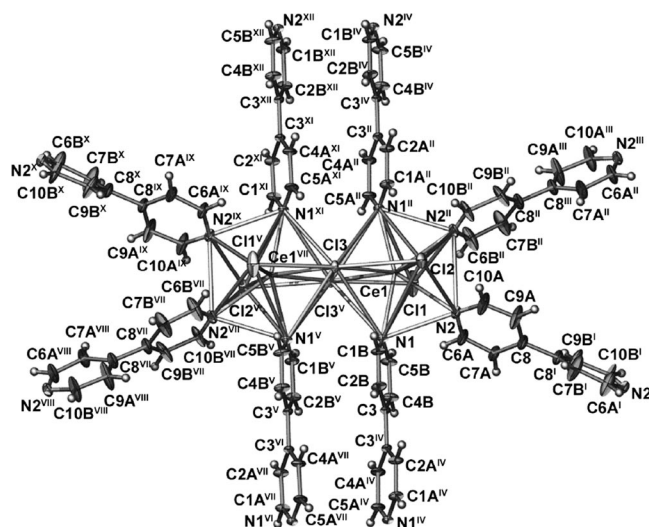


Figure 1. Extended dimeric unit of $\frac{2}{3}[\text{Ce}_2\text{Cl}_6(4,4'\text{-bipy})_4]\cdot\text{py}$. The thermal ellipsoids depict 30% of the probability level of the atoms. Symmetry operations: ^I3/2 −*x*, 1/2 −*y*, −*z*; ^{II}*x*, −*y*, *z*; ^{III}3/2 −*x*, *y*−1/2, −*z*; ^{IV}*x*, 1 −*y*, *z*; ^V1−*x*, *y*, 1 −*z*; ^{VI}1−*x*, 1 −*y*, 1 −*z*; ^{VII}1−*x*, *y*, 1−*z*; ^{VIII}*x*−1/2, *y*−1/2, 1+*z*; ^{IX}1−*x*, −*y*, 1 −*z*; ^X*x*−1/2, *y*−1/2, 1+*z*; ^{XI}1−*x*, −*y*, 1 −*z*; ^{XII}1−*x*, *y*−1, 1 −*z*.

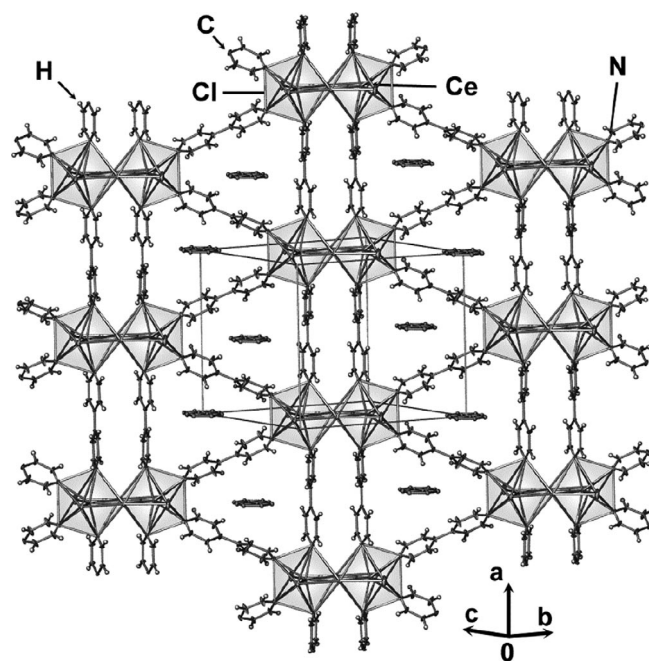


Figure 2. Crystal structure of $\frac{2}{3}[\text{Ce}_2\text{Cl}_6(4,4'\text{-bipy})_4]\cdot\text{py}$, showing a two-dimensional sheet structure. The thermal ellipsoids depict 30% of the probability level of the atoms, intercalated pyridine molecules are at disordered positions within cavities.

nitrogen atoms of the 4,4'-bipyridyl ligands that bind to cerium [$\text{Ce1}-\text{N1}, \text{N1}^{\text{I}}$ 262.8(2) pm, $\text{Ce1}-\text{N2}, \text{N2}^{\text{I}}$ 283.7(2) pm] are also positioned on a plane perpendicular to the Ce_2Cl_6 plane. Each nitrogen atom belongs to a μ_2 -bridging 4,4'-bipyridine molecule, which interconnects the dimeric Ce_2Cl_6 units to a two-dimensional network (Figure 2). Two distinct 4,4'-bipyridine molecules connect the Ce_2Cl_6 dimers along the *a* axis perpendicular to the lanthanide–chloride plane. The distance between the longitudinal axes of both 4,4'-bipyridine molecules is

378.9(3) pm, revealing parallel-displaced π - π repulsion of the aromatic pyridyl pairs. These ladder-like strands are diagonally connected via two 4,4'-bipyridine molecules per SBU forming trigonal cavities within the sheet network. The topology was determined via TOPOS^[16] counting 4,4'-bipyridine and the double chloride bridge as normal bridges and the Ce^{III} ions as network nodes (Figure 3 top). Determination revealed an Archimedean *cem* topology type.

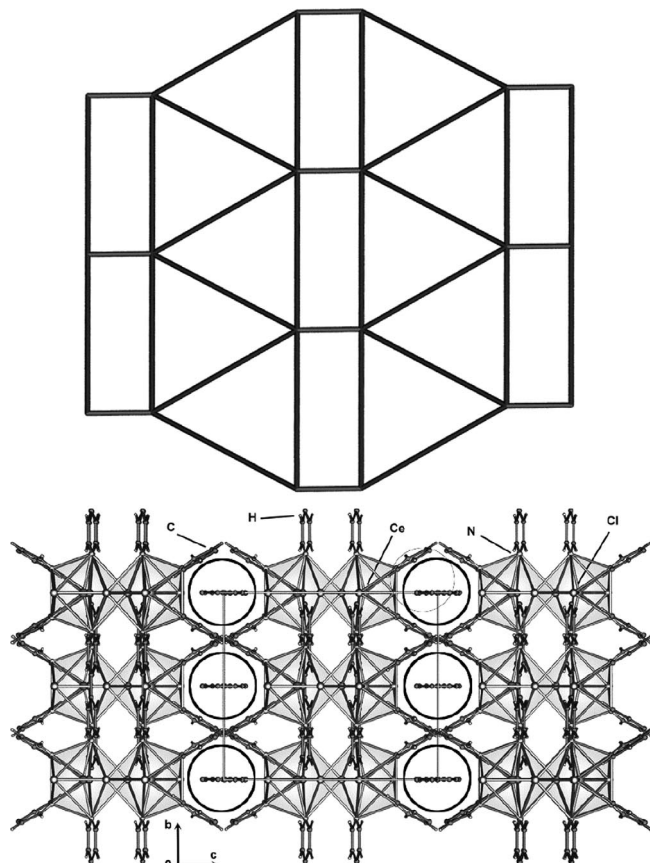


Figure 3. Depiction of the Archimedean *cem* topology type of the $\frac{2}{3}[\text{Ce}_2\text{Cl}_6(4,4'\text{-bipy})_4]$ network (top). View along *a* axis revealing the channel like structures (black circles) through overlaying network sheets of $\frac{2}{3}[\text{Ce}_2\text{Cl}_6(4,4'\text{-bipy})_4]$ (bottom).

The point symbol for the uninodale 5-c network $\frac{2}{3}[\text{Ce}_2\text{Cl}_6(4,4'\text{-bipy})_4]$ and the corresponding Ce³⁺ ions is $\{3^3.4^4.5^3\}^{[17]}$ with a Vertex symbol of $[3.3.3.4.4.*]$ and the ring types are $[3a.3a.3a.4a.4a.*]$ (the asterisk marks calculated ring circulations above 20 that were omitted). Analogous networks with *cem* topology can be found in transition metal MOFs based on carboxy ligands like $\frac{2}{3}[\text{Cd}(\text{Hpptpz})(\text{bpba})\cdot 2\text{H}_2\text{O}]^{[18]}$ and $\frac{2}{3}[\text{Co}(1,2\text{-phda})(4\text{-bpmp})_{1.5}(\text{H}_2\text{O})]^{[19]}$. The sheets are alternately stacked along $[101]$ perpendicular to their proliferation plane along (201) . The alternating stacking between two sheets can be best described with half an elemental cell displacement along the *b* axis for the Ce₂Cl₆ dimeric units. This alignment leads to a formation of a channel like structure along the *a* axis formed by trapezoid like cavities of the sheets. Pyridine molecules are intercalated in every second cavity between the sheets (Figure 3, bottom). The cavities in between the layer

sheets are filled with pyridine molecules, which have two different preferred orientations. Platon^[20] calculations reveal a theoretically accessible void volume of $2415 \text{ pm}^3 \times 10^6$ correlating to 19.1% unit cell volume.

X-ray powder diffraction investigations reveal good accordance of the observed powder diffractogram with the simulated diffractogram based on single-crystal data (Figure 4). Furthermore, about one percent of unreacted CeCl₃ can be observed in the diffractogram and was determined by the Rietveld-refinement using TOPAS.^[21]

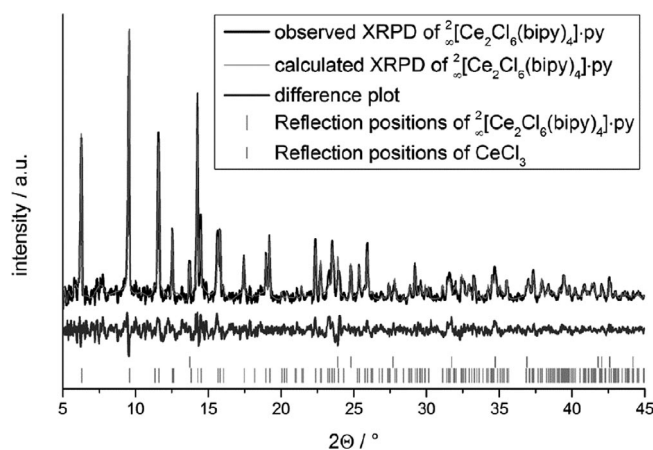


Figure 4. Rietveld-plot of the observed X-ray powder diffractogram of $\frac{2}{3}[\text{Ce}_2\text{Cl}_6(\text{bipy})_4]\cdot\text{py}$ with a combined fit of the Ce network (bottom) and CeCl₃ (above).

Photoluminescence and IR Spectroscopy

The two-dimensional network $\frac{2}{3}[\text{Ce}_2\text{Cl}_6(\text{bipy})_4]\cdot\text{py}$ shows interesting photoluminescence properties with Ce³⁺-centred light-emission in the UV-blue range below the visible border. Determinations via photoluminescence spectroscopy (Figure 5) reveal a broad band emission in the range of $\lambda = 330\text{--}380 \text{ nm}$, which can be correlated to the fluorescent Ce³⁺ $5d^1 \rightarrow 4f^1$ transition. Furthermore, the split emission profile with two maxima at $\lambda_{\text{max}} = 336 \text{ nm}$ and 360 nm can be correlated to the splitting of the ground level into $^2F_{7/2}$ and $^2F_{5/2}$ levels due to spin-orbit coupling. The $5d^1 \rightarrow 4f^1$ transition is strongly influenced by the crystal and ligand field as well as the nephelauxetic effect caused by the coordinated chloride anions. The influence of the chloride ions in the coordination sphere of the cerium ion leads to a shift in the energetic position of the lowest $5d^1$ excited state to ca. $32,000 \text{ cm}^{-1}$. Related energies and similar splitting of the emission could be observed for CeCl₃ doped in NaCl, exhibiting the same two maxima in emission at wavelengths with slightly lower energy ($\lambda_{\text{max}} = 346 \text{ nm}$ and 373 nm).^[22] The emission can clearly be addressed to the cerium content of the network $\frac{2}{3}[\text{Ce}_2\text{Cl}_6(\text{bipy})_4]\cdot\text{py}$. An energy diagram as well as a structure-property graphic is also shown in Figure 5. The excitation spectrum exhibits a maximum at $\lambda_{\text{max}} = 284 \text{ nm}$, which can be correlated to the $4f^1 \rightarrow 5d^1$ transition and a shoulder at $\lambda < 250 \text{ nm}$. The excitation maxima at $\lambda < 250 \text{ nm}$ may be correlated to the coordinated 4,4'-bipyridine molecules as the free ligand shows a similar excitation spectrum in this wavelength range. An actual formation of a pos-

sible antenna effect^[23] between 4,4'-bipyridine and Ce³⁺ cannot be proven as the referring excitation band in the range of 300–350 nm correlating to 4,4'-bipyridine is within the shoulder of Ce transitions in the excitation spectrum of $\frac{2}{3}[\text{Ce}_2\text{Cl}_6(4,4'\text{-bipy})_4]$. Typically, these excitation bands can be observed for antenna triggered 4f-4f luminescence of Ln³⁺ ions in compounds based on LnCl₃-4,4'-bipy and py.^[11c,17]

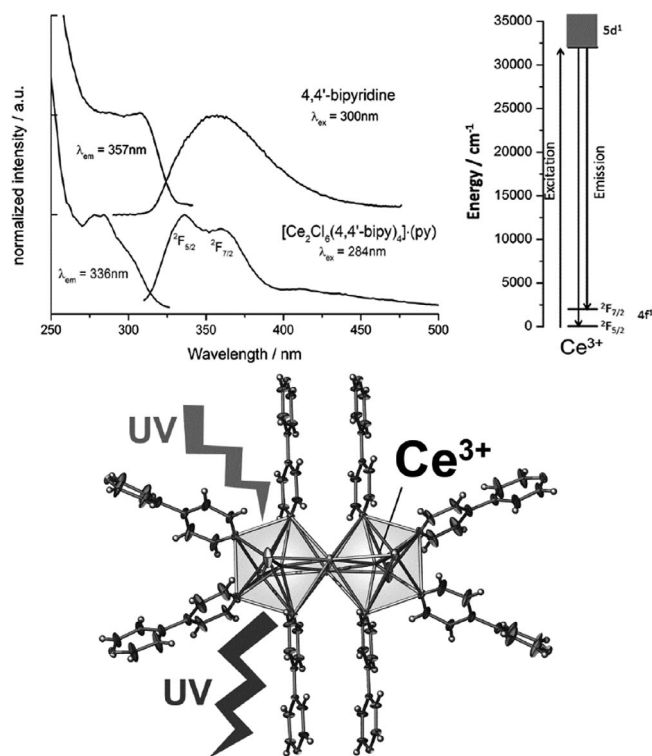


Figure 5. Excitation and emission spectra of 4,4'-bipyridine and $\frac{2}{3}[\text{Ce}_2\text{Cl}_6(4,4'\text{-bipy})_4]$ in the solid-state (top, left); the 5d¹–4f¹ transitions from the excited state 5d¹ to the split ground state are marked in the graphics by the term symbols. Energy diagram of the cerium(III)-centred luminescence (top, right). Schematic diagram of the structure-luminescence coherence (bottom).

Mid IR spectra of the product confirm the coordination of 4,4'-bipyridine to the Ce³⁺ ion by a shift of the ν(C=N) ring vibration node from 1591 cm⁻¹ for the free molecule to 1602 cm⁻¹ for the metal-bonded molecule in the network. Furthermore, the IR band at 1483 cm⁻¹ confirms the presence of pyridine intercalated into the cavities of the sheet structure.

Conclusions

The 2D network $\frac{2}{3}[\text{Ce}_2\text{Cl}_6(\text{bipy})_4]\cdot\text{py}$ was synthesized and characterized as the missing link between the 2D MOFs $\frac{2}{3}[\text{Ln}_2\text{Cl}_6(\text{bipy})_3]\cdot 2\text{bipy}$ (Ln = Pr – Tb) and the dense 3D framework $\frac{2}{3}[\text{La}_2\text{Cl}_6(\text{bipy})_5]\cdot 4\text{bipy}$. As crystallization directly from a melt of bipy failed, a solvent assisted solvothermal approach in pyridine was used to circumvent this problem. The cerium containing network marks a real intermediate between La and Pr regarding the coordination number and its crystal structure that does not adopt one of the known phases, while the assisting solvent is not involved in coordination. Moreover,

the 2D network shows intense UV emission of allowed Ce³⁺ transitions 5d¹→4f¹ (²F_{7/2}, ²F_{5/2}) at 336 nm and 360 nm representing a ligand and crystal field based splitting of the 5d-states, with the lowest energy levels being close to the visible range.

Experimental Section

All manipulations were carried out in an inert atmosphere using glove box, ampoule as well as Schlenk and Young vacuum line techniques. The IR spectra were recorded with a THERMO NICOLET 380 spectrometer. IR investigations were done with KBr pellets under vacuum. Thermal properties were determined by simultaneous DTA/TG (NETZSCH STA 409) in a constant argon and nitrogen flow of 20 ml·min⁻¹. Micro analysis was carried out with an ELEMENTAR vario micro cube. Anhydrous CeCl₃ was prepared by a modified ammonium halide route.^[24] Hereby, high temperature calcined CeO₂ (99.9%, Auer-Remy) was dissolved by boiling in concentrated acids HCl (37%, fuming)/HNO₃ (69%, fuming) and HCl (37%, fuming)/H₂O₂ (30%). Colorless, pure Ce(OH)₃ was obtained by alkaline precipitation with concentrated aqueous NaOH solution (37%). Alternatively, Cerium hydroxide was obtained by alkaline treatment of an aqueous Ce(NO₃)₃·6(H₂O) (99%, Riedel-deHaën) solution. The corresponding precipitates were dissolved in HCl acid (10 mol·L⁻¹, reagent grade) and NH₄Cl (99.9%, Fluka) was added. (NH₄)₃CeCl₆ was formed and decomposed at 500 °C under vacuum, followed by purification by sublimation under vacuum at 850 °C yielding anhydrous CeCl₃. 4,4'-bipyridine (98%, Acros) was dried under vacuum prior to reaction, and anhydrous pyridine (99%, Acros) was used as purchased.

Synthesis of $\frac{2}{3}[\text{Ce}_2\text{Cl}_6(\text{bipy})_4]\cdot\text{py}$: CeCl₃ (148 mg, 0.6 mmol), 4,4'-bipyridine (4,4'-bipy, C₁₀N₂H₈; 234 mg, 1.5 mmol), and pyridine (py, C₅NH₅; 491 mg, 6.2 mmol) were sealed in an evacuated (3 × 10⁻³ mbar) DURAN® glass ampoule. A heating program of six steps was applied starting with heating to 50 °C with a rate of 5 K·h⁻¹, additional heating to 100 °C with 1 °C·h⁻¹, and then to 130 °C with 0.5 °C·h⁻¹. The temperature was maintained for 168 h followed by reducing to 100 °C with a rate of 0.5 °C·h⁻¹ and to room temperature with 1 °C·h⁻¹. The reaction yielded a yellowish crystalline powder within the saturated solvent. Alternatively, the reaction can also be carried out at 220 °C (starting with heating to 120 °C at 10 °C·h⁻¹ and further heating to 220 °C at 2 °C·h⁻¹). The temperature was maintained for 168 h then lowered down to 120 °C at 2 °C·h⁻¹ and to room temperature at a rate of 1 °C·h⁻¹ leading to the same product, which was confirmed by X-ray diffraction. The compound was washed two times with 1 mL anhydrous pyridine to remove excess 4,4'-bipyridine and dried in a vacuum. Yield: 179 mg (50%). The product is air and moisture sensitive. Vibrational spectroscopy MIR (KBr): $\tilde{\nu} = \nu(\text{C-H})$ 3050 w, 2921 w, 2852 w, ν(C–N ring, 4,4'-bipy) 1602 vs, ν(C–C ring) 1532 w, 1413 m, 1139 w, 1073 w, δ(C–H, pyridine) 1438 w, δ(C–H) 1488 w, 1322 vw, 1262 vw, 1224 m, ν(C=C, aromatic) 1002 w, γ(C–H) 854 vw, 808 vs, 759 vw, δ(C=C, aromatic) 1042 w, 1110 w, 732 vw, 704 m, 618 s, 570 vw, 518 vw, 417 w, γ(C=C, aromatic) 465 vw, 443 vw, 485 w cm⁻¹. $\frac{2}{3}[\text{Ce}_2\text{Cl}_6(\text{bipy})_4]\cdot\text{py}$ (1196.91 g·mol⁻¹): C 44.96 (calcd. 45.16); H 3.15 (3.16); N 10.48 (10.53)%.

Crystal Structure Determination, Powder X-ray Diffraction, and Photoluminescence Spectrometry: Suitable crystals of $\frac{2}{3}[\text{Ce}_2\text{Cl}_6(4,4'\text{-bipy})_4]\cdot\text{py}$ for single-crystal X-ray analysis were selected under viscous perfluorinated polyalkylether (ABCER). The data collection was carried out with a BRUKER AXS SMART APEX diffractometer equipped with graphite monochromator at 168 K and Mo-K_α radiation (λ = 71.07 pm) using the BRUKER AXS SMART Soft-

ware package.^[25] Multi-scan absorption via SADABS was applied.^[26] Further data processing was done with XPREP. Structure solution was achieved with the Patterson method^[27] using SHELXS-97. The compound crystallizes in the monoclinic space group *C2/m*. All non-hydrogen atoms were refined anisotropically by least-squares techniques (SHELXL-97).^[28] All hydrogen atoms were calculated into pre-set positions with isotropic thermal parameters adjusted to 1.2 of the corresponding carbon atom. The crystallographically independent pyridyl rings of the coordinated 4,4'-bipyridine molecules show rotational disorder along their longitudinal axis, which was refined in two distinct positions for each ring; the referring C20–C24 were thereby refined isotropically. Furthermore, the intercalated pyridine molecule exhibits positional disorder along the longitudinal axis, which was refined by two isotropic benzene rings without hydrogen atoms. Lower symmetry does not overcome the disorder, which may be the result of a domain twinning. Integrity of symmetry was checked and no higher symmetry could be found.^[20] For further crystallographic information see Table 1.

Crystallographic data (excluding structure factors) for the structure in this paper have been deposited with the Cambridge Crystallographic Data Centre, CCDC, 12 Union Road, Cambridge CB21EZ, UK. Copies of the data can be obtained free of charge on quoting the depository number CCDC-988091 (Fax: +44-1223-336-033; E-Mail: deposit@ccdc.cam.ac.uk, <http://www.ccdc.cam.ac.uk>).

$[\text{Ce}_2\text{Cl}_6(\text{bipy})_4]\cdot\text{py}$ was also investigated on powder samples in sealed Lindeglas capillaries on a BRUKER AXS D8 Discover powder X-ray diffractometer, equipped with Lynx-Eye detector in transmission geometry. X-ray radiation ($\text{Cu}-K_{\alpha 1}$; $\lambda = 154.06 \text{ pm}$) was focused with a Goebel mirror, $\text{Cu}-K_{\alpha 2}$ radiation was eliminated by the application of a Ni absorber. Diffraction patterns were recorded and analyzed using the BRUKER AXS Diffrac-Suite. Refinement of lattice parameters, atom positions and content of CeCl_3 was achieved via the Rietveld-method with TOPAS,^[21] using the fundamental parameters approach as reflection profiles (convolution of appropriate source emission profiles with axial instrument contributions as well as crystallite microstructure effects).

Excitation and emission spectra were recorded with a HORIBA Jobin Yvon Spex Fluorolog 3 spectrometer equipped with a 450 W Xe-lamp, double grating excitation and emission monochromators and a photo multiplier tube (R928P) at room temperature using the FluorEssence software. Excitation spectra were corrected for the spectral distribution of the lamp intensity using a photodiode reference detector. Additionally, both excitation and emission spectra were corrected for the spectral response of the monochromators and the detector using correction spectra provided by the manufacturer. All samples were investigated as solids in spectroscopically pure quartz cuvettes in front face mode at room temperature.

Acknowledgements

We gratefully acknowledge the Deutsche Forschungsgemeinschaft for supporting this work and the Evangelisches Studienwerk Villigst e.V. for Ph.D. scholarship funding *P. R. Matthes*.

References

- [1] S. R. Batten, N. R. Champness, X.-M. Chen, J. Garcia-Martinez, S. Kitagawa, L. Öhrstöm, M. O'Keeffe, M. P. Suh, J. Reedijk, *Pure Appl. Chem.* **2013**, *85*, 1715.
- [2] a) S. Kitagawa, R. Kitaura, S. Noro, *Angew. Chem.* **2004**, *116*, 2388–2430; b) S. Kitagawa, R. Kitaura, S. Noro, *Angew. Chem. Int. Ed.* **2004**, *43*, 2334.

- [3] M. Kurmoo, *Chem. Soc. Rev.* **2009**, *38*, 13530.
- [4] a) M. D. Allendorf, C. A. Bauer, R. K. Bhakta, R. J. T. Houk, *Chem. Soc. Rev.* **2009**, *38*, 1330; b) Y. Cui, Y. Yue, G. Qian, B. Chen, *Chem. Rev.* **2012**, *112*, 1126; c) J. Heine, K. Müller-Buschbaum, *Chem. Soc. Rev.* **2013**, *42*, 9232; d) J. Rocha, L. D. Carlos, F. A. A. Paz, D. Ananias, *Chem. Soc. Rev.* **2011**, *40*, 926; e) L. V. Meyer, F. Schönfeld, K. Müller-Buschbaum, *Chem. Commun.* **2014**, *50*, 8093.
- [5] A. U. Czaja, N. Trukhan, U. Müller, *Chem. Soc. Rev.* **2009**, *38*, 1284.
- [6] L. E. Kreno, K. Leong, O. K. Farha, M. Allendorf, R. P. V. Duyne, J. T. Hupp, *Chem. Rev.* **2012**, *112*, 1105.
- [7] A. Zurawski, M. Mai, D. Baumann, C. Feldmann, K. Müller-Buschbaum, *Chem. Commun.* **2011**, *47*, 496.
- [8] a) V. S. Dhanya, M. R. Sudarsanakumar, S. Suma, S. W. Ng, M. S. Augustine, S. M. Roy, *Inorg. Chem. Commun.* **2013**, *35*, 140; b) C. A. F. de Oliveira, F. F. da Silva, I. Malvestiti, V. Rodrigues dos S. Malta, J. D. L. Dutra, N. B. da Costa Jr., R. O. Freire, S. Alves Jr., *J. Mol. Struct.* **2013**, *1041*, 61; c) S.-F. Weng, Y.-H. Wang, C.-S. Lee, *J. Solid State Chem.* **2012**, *188*, 77; d) Y. Gao, Y. Xu, Z. Han, C. Li, F. Cui, Y. Chi, C. Hu, *J. Solid State Chem.* **2010**, *183*, 1000.
- [9] A. Zurawski, J.-C. Rybak, L. V. Meyer, P. R. Matthes, V. Stepanenko, N. Dannenbauer, F. Würthner, K. Müller-Buschbaum, *Dalton Trans.* **2012**, *41*, 4067.
- [10] a) C. J. Höller, K. Müller-Buschbaum, *Inorg. Chem.* **2008**, *47*, 10141; b) C. J. Höller, P. R. Matthes, M. Adlung, C. Wickleder, K. Müller-Buschbaum, *Eur. J. Inorg. Chem.* **2012**, 5479.
- [11] a) C. J. Höller, P. R. Matthes, J. Beckmann, K. Müller-Buschbaum, *Z. Anorg. Allg. Chem.* **2010**, *636*, 395; b) C. J. Höller, M. Mai, C. Feldmann, K. Müller-Buschbaum, *Dalton Trans.* **2010**, *39*, 461; c) P. R. Matthes, C. J. Höller, M. Mai, J. Heck, S. J. Sedlmaier, S. Schmiechen, C. Feldmann, W. Schnick, K. Müller-Buschbaum, *J. Mater. Chem.* **2012**, *22*, 10179.
- [12] K. Binnemans, *Chem. Rev.* **2009**, *109*, 4283.
- [13] a) J.-S. Li, B. Neumüller, K. Dehnicke, *Z. Anorg. Allg. Chem.* **2002**, *628*, 45–50; b) W. J. Evans, D. G. Giarikos, J. W. Ziller, *Organometallics* **2001**, *20*, 5751; c) G. B. Deacon, N. M. Scott, B. W. Skelton, A. H. White, *Z. Anorg. Allg. Chem.* **2006**, *632*, 1945.
- [14] S. Kano, H. Nakano, M. Kojima, N. Baba, K. Nakajima, *Inorg. Chim. Acta* **2003**, *349*, 6.
- [15] J. Lhoste, N. Henry, T. Loiseau, F. Abraham, *Polyhedron* **2011**, *30*, 1289.
- [16] V. A. Blatov, A. P. Shevchenko, *TOPOS 4.0*, **2011**.
- [17] P. R. Matthes, J. Nitsch, A. Kuzmanoski, C. Feldmann, T. B. Marder, K. Müller-Buschbaum, *Chem. Eur. J.* **2013**, *19*, 17369.
- [18] D. Sun, L.-L. Han, S. Yuan, Y.-K. Deng, M.-Z. Xu, D.-F. Sun, *Cryst. Growth Des.* **2013**, *13*, 377.
- [19] K. M. Blake, L. L. Johnson, J. H. Nettleman, R. M. Supkowski, R. L. LaDuca, *CrystEngComm* **2010**, *12*, 1927.
- [20] A. L. Spek, *J. Appl. Crystallogr.* **2003**, *36*, 7–13.
- [21] A. Coelho, V. TOPAS-ACADEMIC, Coelho Software, Brisbane, Australia, **2007**.
- [22] A. S. Voloshinovskii, V. V. Visovskiy, G. B. Stryganyuk, A. S. Pushak, T. S. Malyy, O. T. Antonyak, Z. A. Khapko, *J. Phys. Condens. Matter* **2008**, *20*, 325218.
- [23] S. I. Weissman, *J. Chem. Phys.* **1942**, *10*, 214.
- [24] G. Meyer, *Inorg. Synth.* **1989**, *25*, 146.
- [25] Bruker, *SMART Apex Suite 2001*, Bruker AXS Inc., Madison, Wisconsin, USA.
- [26] Bruker, *SADABS 2001*, Bruker AXS Inc., Madison, Wisconsin, USA.
- [27] A. L. Patterson, *Z. Kristallogr. A* **1935**, *90*, 517.
- [28] G. M. Sheldrick, *Acta Crystallogr., Sect. A* **2007**, *64*, 112.

Received: August 6, 2014
 Published Online: October 9, 2014